

MICROSCOPIC MODEL ANALYSIS OF THE ${}^6\text{He}$, ${}^6\text{Li} + {}^{28}\text{Si}$ TOTAL REACTION CROSS SECTIONS AT THE ENERGY RANGE 5-50 A MEV

K. V. LUKYANOV, I. N. KUKHTINA, V. K. LUKYANOV,
Yu. E. PENIONZHKEVICH, Yu. G. SOBOLEV, E. V. ZEMLYANAYA

Joint Institute for Nuclear Research, Dubna 141980, Russia

Abstract

The existing and some preliminary experimental data on the total cross sections of the ${}^4,6\text{He}$, ${}^6,7\text{Li} + {}^{28}\text{Si}$ reactions at energies $E=5-50$ A MeV are demonstrated. The data on ${}^6\text{Li}, {}^6\text{He} + {}^{28}\text{Si}$ are analyzed in the framework of the microscopic optical potential with real and imaginary parts obtained with a help of the double-folding procedure and by using the current models of densities of the projectile nuclei. Besides, the microscopic double-folding Coulomb potential is calculated and its effect on cross sections is compared with that when one applies the traditional Coulomb potential of the uniform charge distribution. The semi-microscopic potentials are constructed from both the renormalized microscopic potentials and their derivatives to take into account collective motion effect and to improve an agreement with experimental data.

1 Introduction

Generally, the aim of our study is to analyze the possibility of the microscopic optical potential to give a physical interpretation of the total reaction cross sections of ${}^4,6\text{He}$, ${}^6,7\text{Li}$ on ${}^{28}\text{Si}$ (see refs. [1]-[5]) including some preliminary data on the ${}^6\text{Li} + {}^{28}\text{Si}$ reaction at the energies $E=5-50$ A MeV (see Fig. 1), and at present we study only the ${}^6\text{He}, {}^6\text{Li} + {}^{28}\text{Si}$ cross section. There is the following motivation of this task. First, an interpretation of experimental data with a help of usually applied phenomenological optical potentials does not answer questions both on the nuclear structure of colliding nuclei and on the mechanism of their scattering. Moreover, such kind of fitting is, in fact, only the parametrization of data by introducing a set, say, of the six or more free parameters, which are different for different energies and kinds of interacting nuclei.

Otherwise, the microscopic models do not contain free parameters and provide the possibility to test the models of nuclear structure. Particularly, in this paper we use the current models of the projectile nuclei ${}^6\text{He}$ and ${}^6\text{Li}$ to estimate a sensitivity of total cross sections to a behavior of their densities in the peripheral region. In calculations, we use the Tanihata model [6] and the cluster-orbital shell-model approximation (COSMA) [7] of density distributions of bare protons (Z) and neutrons (N) in nuclei

$$\rho_X(r) = \frac{2}{(\bar{a}\sqrt{\pi})^3} e^{-(r/\bar{a})^2} + \frac{X-2}{3} \frac{2}{(\bar{b}\sqrt{\pi})^3} \left(\frac{r}{\bar{b}}\right)^2 e^{-(r/\bar{b})^2}, \quad X = Z, N, \quad (1.1)$$

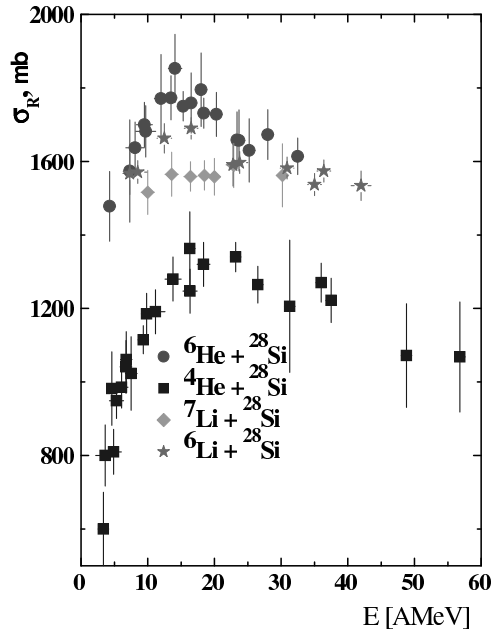


Figure 1: The total reaction cross sections measured in [1]-[5].

where \bar{a} , \bar{b} are parameters of the models. Also, densities of the large-scale shell-model (LSSM) [8] is also presented together with the ${}^6\text{Li}$ density from Tables of [9]. In Fig. 2 one sees the visual distinction of shapes of the proton, neutron and the nuclear matter densities obtained in these models. Between these densities only the LSSM has the realistic exponential behavior at large distances while the others have the Gaussian shape of tails.

In Sec. 2, the double-folding model (see, e.g., [10]), including the exchange term, is applied to calculate the real part of the microscopic optical potential whereas for its imaginary part we takes the form obtained in [11] basing on high-energy approximation (HEA) theory of scattering [12, 13]. Applications of the microscopic potentials are made in Sec. 3. The role of the Coulomb potential is also analyzed by comparison of cross sections calculated with the traditional Coulomb potential of the uniform charge density distribution, and with that obtained in the framework of folding procedure accounting for the realistic nuclear charge density distributions. Then, we discuss the method of adding free parameters to account for influence of collective modes of nuclei. Summary and conclusion are done in Sec. 4.

2 Microscopic optical potential

The double-folding nucleus-nucleus potential (the real one) consists of the direct and exchange parts:

$$V^{DF} = V^D + V^{EX} \quad (2.2)$$

$$V^D(r) = \int d^3r_p d^3r_t \rho_p(\mathbf{r}_p) \rho_t(\mathbf{r}_t) v_{NN}^D(s), \quad \mathbf{s} = \mathbf{r} + \mathbf{r}_t - \mathbf{r}_p, \quad (2.3)$$

$$V^{EX}(r) = \int d^3r_p d^3r_t \rho_p(\mathbf{r}_p, \mathbf{r}_p + \mathbf{s}) \rho_t(\mathbf{r}_t, \mathbf{r}_t - \mathbf{s}) \times$$

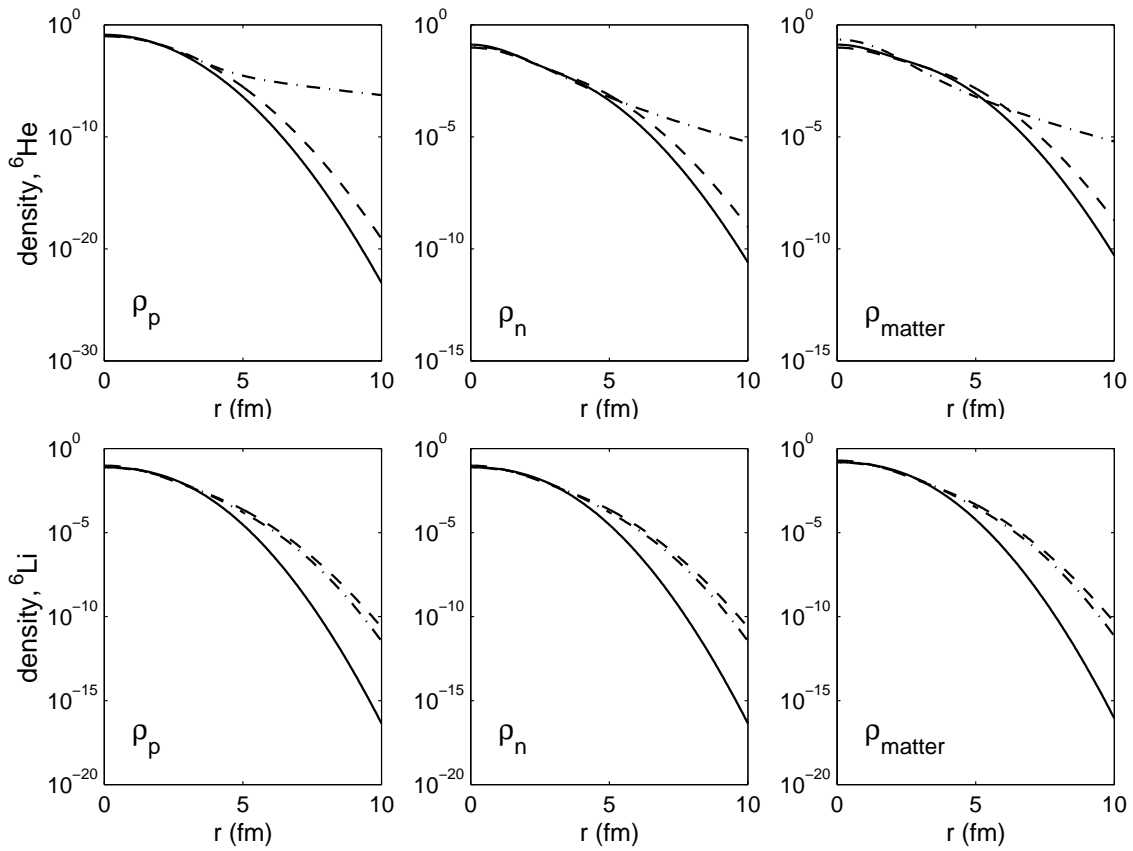


Figure 2: Density distributions of ${}^6\text{He}$ and ${}^6\text{Li}$, calculated in different models. Solid curves: Tanihata (${}^6\text{He}$) and table (${}^6\text{Li}$); dash-dotted: LSSM; dashed: COSMA (see the text)

$$\times v_{NN}^{EX}(s) \exp\left[\frac{i\mathbf{K}(r) \cdot s}{M}\right], \quad (2.4)$$

where $\rho_{p,t}$ are the one-particle projectile (p) and target (t) matrices of densities. The modern calculations usually apply the effective Paris nucleon-nucleon CDM3Y6 potential v_{NN} having the form

$$v_{NN}(E, \rho, s) = g(E) F(\rho) v(s), \quad v(s) = \sum_{i=1,2,3} N_i \frac{\exp(-\mu_i s)}{\mu_i s}, \quad (2.5)$$

where the energy and density dependencies are given as

$$g(E) = 1 - 0.003E/A_p, \quad F(\rho) = C \left[1 + \alpha \exp(-\beta\rho) - \gamma\rho\right], \quad \rho = \rho_p + \rho_t, \quad (2.6)$$

$$C = 0.2658, \quad \alpha = 3.8033, \quad \gamma = 4.0,$$

and the parameters N_i and μ_i are done in [10]. The energy dependence of V^{EX} arises primarily from the contribution the exponential in the integrand, where $K(r) = \{2Mm/\hbar^2[E - V_N^{DF}(r) - V_c(r)]\}^{1/2}$ is the local nucleus-nucleus momentum, $M = A_p A_t / (A_p + A_t)$, m is the nucleon mass, and therefore there occurs the typical non-linear problem.

Here we paid an attention on the important role of the exchange effect in calculations of nucleus-nucleus real potentials. This is depicted in Fig. 3 where the double-folding V^{DF} -potential for the ${}^6\text{He} + {}^{28}\text{Si}$ scattering at $E=25$ MeV/nucleon is calculated with a help of two

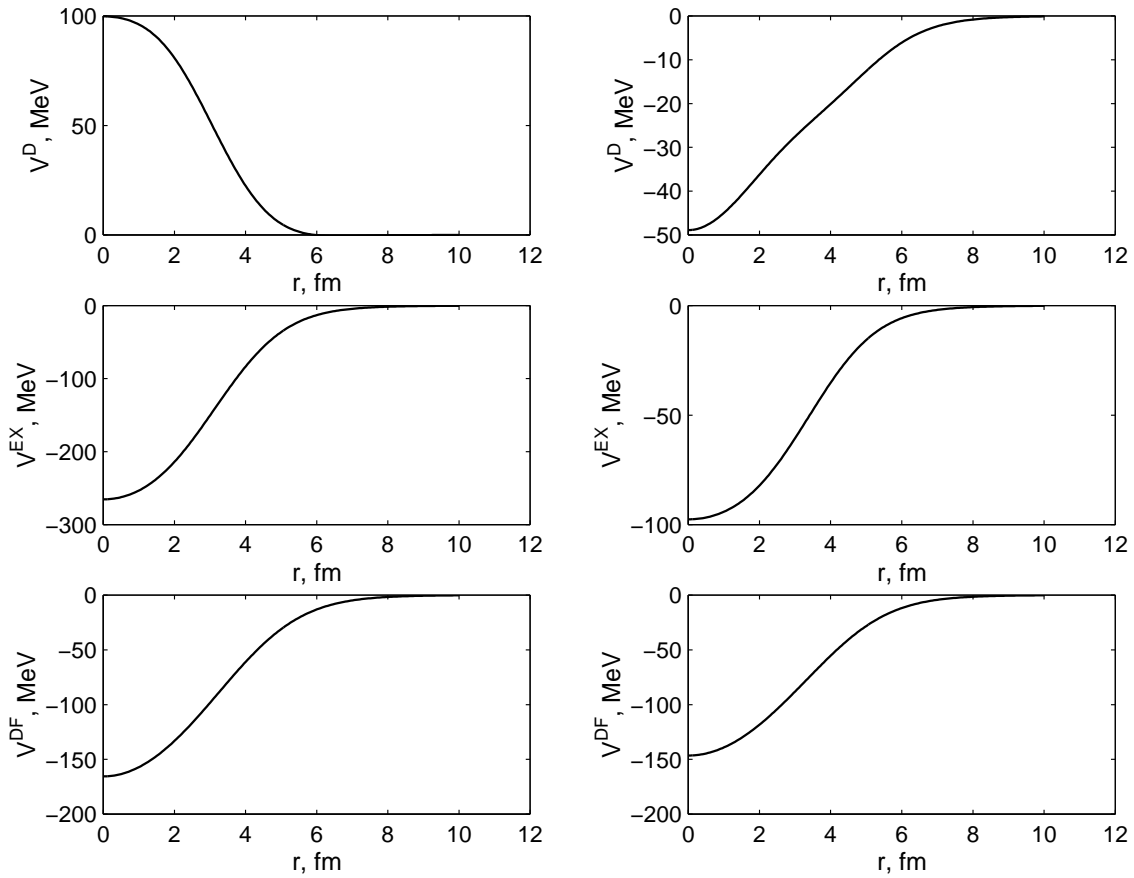


Figure 3: Behavior of different terms and of the total nucleus-nucleus potentials of ${}^6\text{He}+{}^{28}\text{Si}$ calculated with the Paris (left side) and Reid (right side) effective NN-potentials (see the text).

different every so often kinds of effective v_{NN} potentials, the Paris CDM3Y6 and the Reid DDM3Y1 potentials. They have different sets of the parameters N_i , μ_i and C , α , β , γ (see [10]). It is seen, that their direct parts has different signs, and thus the exchange part plays the crucial role in forming the whole nuclear potential.

Note that when constructing microscopic optical potentials people usually use only the real double-folding potential (2.2)-(2.5) while the imaginary part is taken in a phenomenological form with free parameters fitted to experimental data for each specific energy individually. Instead, in our calculations we use below the imaginary part as it is done in the microscopic optical potential (HEA-potential) obtained in [11] basing on the HEA theory [12, 13]. Its imaginary part is as follows:

$$W^H(r) = -\frac{2E}{k(2\pi)^2} \bar{\sigma}_{NN} \int_0^\infty dq q^2 j_0(qr) \tilde{\rho}_p(q) \tilde{\rho}_t(q) \tilde{f}_N(q), \quad (2.7)$$

where $\tilde{\rho}(q) = \int d^3r \exp(i\mathbf{q}\mathbf{r})\rho(r)$ is the form factor of a pointlike nuclear density, and σ_{NN} is the total nucleon-nucleon cross sections that is parametrized in [14] as a function of the NN collision energy. The superscript H indicates the HEA roots of the potential.

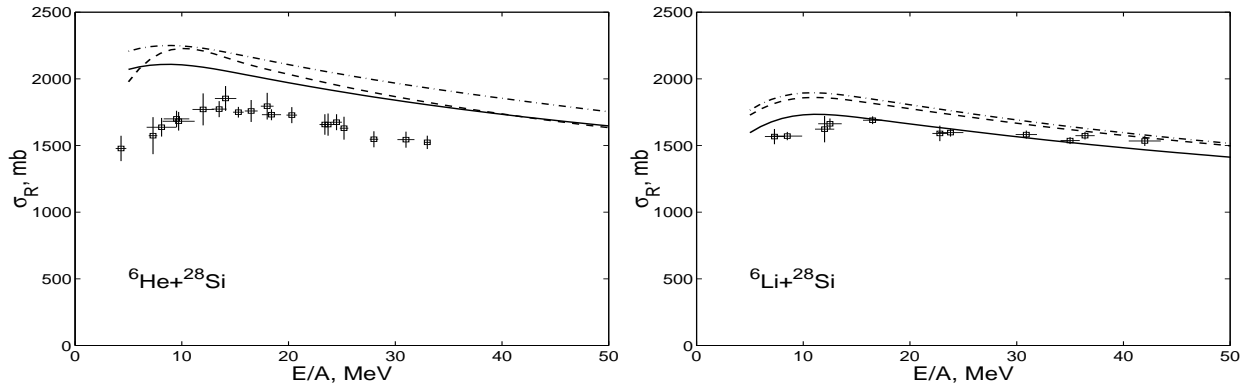


Figure 4: Microscopic calculations of the total cross sections using the microscopic optical potential $V^{DF} + iW^H$ without introducing free parameters. The Paris NN -potential is used. Solid curves: Tanihata density; dashed curves: LSSM; dash-dotted curves: COSMA.

3 Results of the cross section calculations

Fig. 4 exhibits microscopic calculations of the total reaction cross sections based on the given folding potentials (2.3,2.4,2.7) and using density distributions of the projectile nuclei ${}^6\text{He}$ and ${}^6\text{Li}$. It is seen that they exceed the experimental data and their shapes follow to the data at energies higher than 15 Mev/nucleon. Numerical calculations of cross sections were made by using the code DWUCK4 [15].

On the next step of our study, to fit cross sections to the data we renormalize strengths of the real and imaginary parts of the potential

$$U_{opt}(r) = N_r V^{DF} + iN_{im} W^H. \quad (3.8)$$

This procedure is commonly used for the real double-folding potential when one adds the phenomenological imaginary part having itself several free parameters. Contrastingly, in our study, on the first stage, we introduce only two parameters to renormalize strengths of the real V^{DF} and imaginary W^H parts, calculated microscopically. Fig. 5 shows the results for the ${}^6\text{He}+{}^{28}\text{Si}$ cross section when the most realistic LSSM projectile density of ${}^6\text{He}$ was taken in calculations. One sees that the renormalization makes it possible to agree calculations to experimental data at larger energies, whereas a significant discrepancy between the theory and experimental data at lower energies is still unchanged. We also mention that there exist some kind of ambiguity when comparing calculated cross sections with the data. Here we show two nearby curves, the solid one has renormalization parameters $N_r=N_{im}=0.5$, and the dashed one $N_r=1.0$, $N_{im}=0.4$. So, we conclude that in the framework of microscopic "volume potentials" (3.8), the simultaneous explanation of the data in the whole region of measurements is not possible. In this connection, at lower energies, the Coulomb interaction can be thought play a pronounced role in the nuclear reaction mechanism.

So, to get more precise results we computed the Coulomb potential using the microscopic folding formula (2.3) with the realistic charge LSSM density and the NN charge interaction potential $v_C = 1/|s|$. Such Coulomb potential and corresponding cross sections was calculated for the ${}^6\text{He}+{}^{28}\text{Si}$ system and compared to that obtained traditionally with a help of the uniformly distributed charge in the sphere of the radius of the sum of radii of colliding nuclei. On the left side of Fig. 6 we exhibit the both potentials. One sees the visible difference of them in the interior region and their small separation in the peripheral band, while at

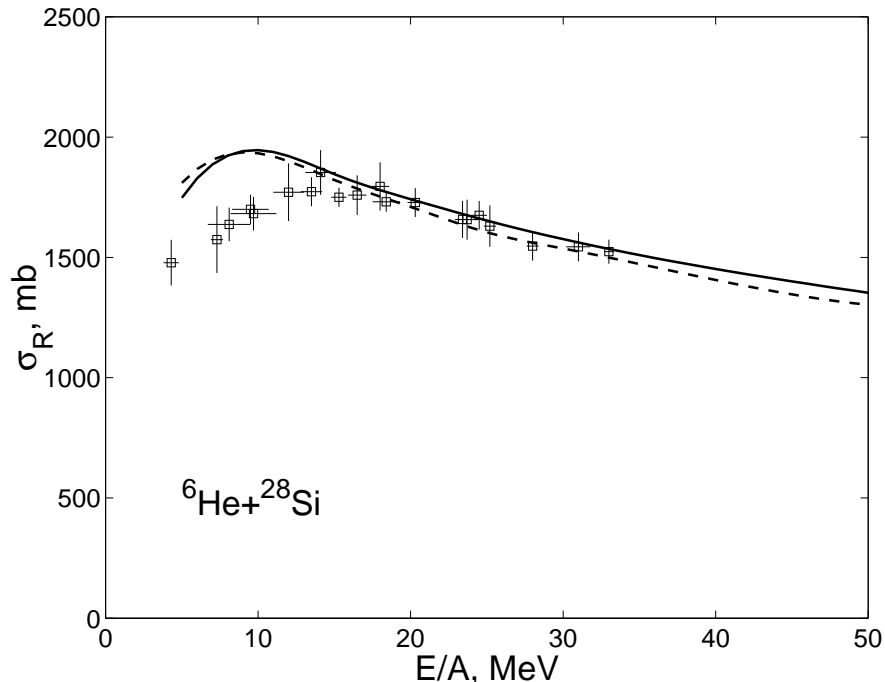


Figure 5: Effect of the strength renormalization of microscopic potentials $N_r V^{DF} + iN_{im} W^H$ on the total reaction cross section. Solid curve: $N_r = N_{im} = 0.5$; dashed curve: $N_r = 1$, $N_{im} = 0.4$.

larger distances they coincide to one another. However this changes do not reveal themselves in behavior of cross sections (right side of Fig. 6), and the “bump” of the ${}^6\text{He}+{}^{28}\text{Si}$ total reaction cross section at $E \simeq 15$ MeV is not explained by correcting the Coulomb potential.

Going step by step in the framework of our goal to study an applicability of microscopic potentials, at this stage we intend to simulate an influence of nuclear collective modes on the mechanism of nucleus-nucleus scattering. It is known from the theory of inelastic scattering that excitations of nuclear collective states can be understood by introducing transition potentials in the form of the derivative of an elastic scattering potential. With respect to this prescription, we add the derivatives ($-rdV/dr$) of our microscopic template potentials (“surface terms”) to construct optical potentials

$$U_{opt}(r) = \left[N_r V^{DF} - N_r^{(1)} r \frac{dV^{DF}}{dr} \right] + i \left[N_{im} W^H - N_{im}^{(1)} r \frac{dW^H}{dr} \right], \quad (3.9)$$

$$U_{opt}(r) = \left[N_r V^{DF} - N_r^{(1)} r \frac{dV^{DF}}{dr} \right] + i \left[N_{im} V^{DF} - N_{im}^{(1)} r \frac{dV^{DF}}{dr} \right], \quad (3.10)$$

Thus, when fitting cross sections to the data we have two else free parameters $N_r^{(1)}$ and $N_{im}^{(1)}$ responsible to the contribution of collective terms. In Fig.7 we demonstrate result of calculations obtained for two kinds of nucleus-nucleus potentials. One of them (left panel) is calculated for the Paris effective NN-potential CDM3Y6 with the LSSM density of ${}^6\text{He}$, and the other one (right panel) is for the Reid BDM3Y2 NN-potential [10] with the FDM-model (functional density method) [16] of density of ${}^6\text{He}$. The fitted coefficients are $N_r=0.7$, $N_r^{(1)}=0.4$, $N_{im}=0.5$, $N_{im}^{(1)}=0.03$ (CDM3Y2 case), and $N_r=1$, $N_r^{(1)}=0.212$, $N_{im}=0.3$, $N_{im}^{(1)}=0.038$ (BDM3Y2 case). It is seen that by introducing derivatives one can get the

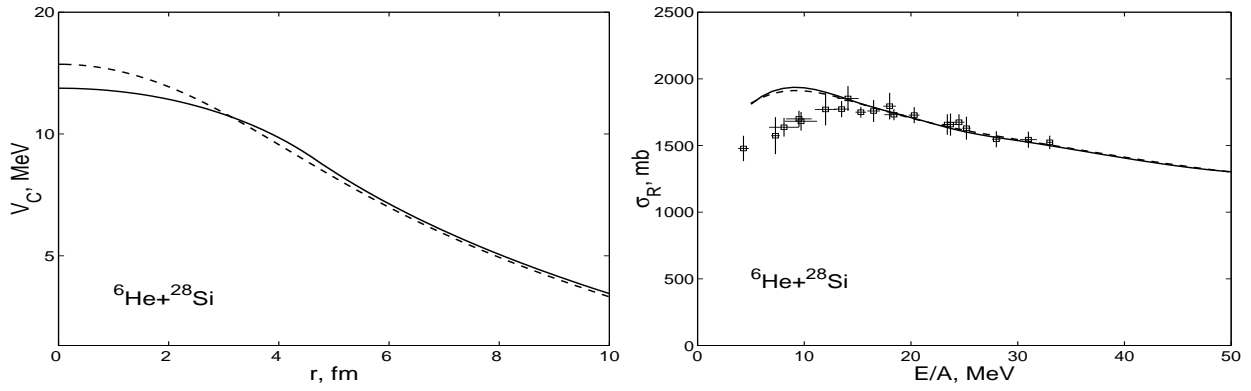


Figure 6: Effect of correcting the Coulomb AA-potential on the total reaction cross section. Left panel: the ordinary (solid) and the corrected (dashed) Coulomb potential for ${}^6\text{He}+{}^{28}\text{Si}$. Right panel: corresponding total cross sections

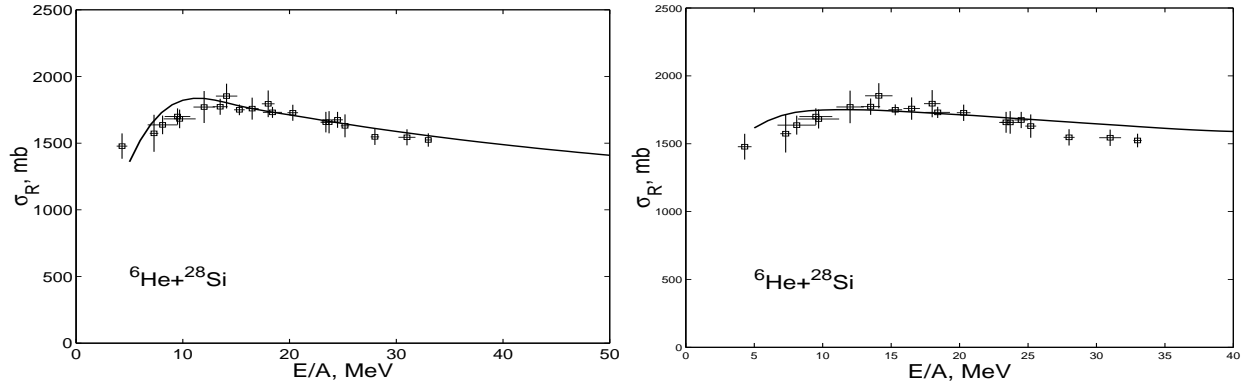


Figure 7: The fit of the four-parameter semi-microscopic potentials with the @surface@ terms to the data when used two microscopic models of the effective NN-forces (see the text).

fairly well agreement with the experimental data in the first case, and the qualitative description for the second potential. These potentials with the "surface terms" have more smooth diffuseness layers as compared to "the volume potentials" (3.8), and this behavior is in correspondence with the models of collective motions of a nuclear surface.

By the way, such semi-microscopic optical potentials need in further improvements to exclude free parameters and to give their fully microscopic interpretation. In this connection, the problem of the physical nature of an enhancement in the ${}^6\text{He}+{}^{28}\text{Si}$ total reaction cross section at about 10 MeV over the Coulomb barrier is still calls for experimental and theoretical investigations. In particular, the study of angular distributions in elastic channel can decrease an ambiguity of parameters of semi-microscopic optical potentials.

4 Summary and conclusion

Microscopic models of nucleus-nucleus optical potentials have no free parameters. They are constructed by using physical characteristics of structure of colliding nuclei and of effective nucleon-nucleon forces in nuclear medium. We considered a possibility of the microscopic

folding potentials to study the total cross sections of reactions ${}^6\text{He}+{}^{28}\text{Si}$ and ${}^6\text{Li}+{}^{28}\text{Si}$. It was shown that a little renormalization of strengths of these potentials by introducing two parameters allow for explain the data at comparably higher energies $E \geq 15$ MeV/nucleon. In this region, the cross sections, calculated with the help of several developed models of the projectile nuclei, are closely related to each other. Simultaneously, it is seen the visible disagreement of these calculations with the lower-energy data, and so that this is the subject of further investigations. Our treatment to use the microscopically calculated Coulomb potential does not improve results at these energies. This turn us to remind that, in general, the ordinary folding potentials take into account only one-particle density distributions of colliding nuclei, and thus effects of another channels, connected with nuclear collective excitations and the nucleon removal reactions, can also play a role in collisions of nuclei. These effects were approximately accounted for by adding the derivatives of the folding potentials to the basic microscopic "volume potential", and as a result, the fairly well agreement was obtained with the data at lower energies. Thus one can conclude that the more developed theory of reactions with exotic beams is called rather than the use of some kind of phenomenological constructions of averaged optical potentials based only on methods of double-folding calculations.

The work was partially supported by RFBR (grant 06-01-00228).

References

- [1] I.V.Kuznetsov, E.Bialkowski, M.P.Ivanov, *et al*, *Phys. At. Nucl.* **65** 1569 (2002).
- [2] M.K.Baktybaev, A.Duisebaev, B.A.Duisebaev, *et al*, *Phys. At. Nucl.* **66**, 1615 (2003).
- [3] V.Yu.Ugryumov, I.V.Kuznetsov, K.B.Basybekov, *et al*, *Nucl. Phys. A* **734**, E53 (2004).
- [4] V.Yu.Ugryumov, I.V.Kuznetsov, E.Bialkowski, *et al*, *Phys. At. Nucl.* **68**, 16 (2005).
- [5] Yu.G.Sobolev, A.Budzanowski, E.Bialkowski, *et al*, *Bull. Rus. Acad.Sc., Physics* **69**,(2005) 1790.
- [6] I.Tanihata, *et al*, *Phys. Lett. B* **289**, 261 (1992).
- [7] M.V.Zhukov, B.V.Danilin, D.V.Fedorov, *et al*, **Phys. Rep.** **231**, 151 (1993).
- [8] S.Karataglidis, P.J.Dortmans, K.Amos, and C.Bennhold, *Phys. Rev. C* **61**, 024319 (2000).
- [9] J.D.Patterson and R.J.Peterson, *Nucl. Phys. A* **717**, 235 (2003).
- [10] D.T.Khoa and G.R.Satchler, *Nucl. Phys. A* **668**, 3 (2000).
- [11] V.K.Lukyanov, E.V.Zemlyanaya, K.V.Lukyanov, *Phys. At. Nucl.* **69**, 240 (2006).
- [12] R.J.Glauber, *Lectures on Theoretical Physics* (Interscience, New York, 1959), p.315.
- [13] A.G.Sitenko, *Ukr. Fiz. Journal* **4**, 152 (1959).
- [14] S.Charagi and G.Gupta, *Phys. Rev. C* **41**, 1610 (1990).
- [15] P.D.Kunz and E.Rost, *Computational Nuclear Physics* V.2 (Eds: Langanke K.et al., Springer Verlag, 1993) p.88.
- [16] O.M.Knyazkov, I.N.Kukhtina, S.A.Fayans, *Phys. At. Nucl.*, **61**, 533 (1998).